



OPEN

Parameter study of the high temperature MOCVD numerical model for AlN growth using orthogonal test design

Jiadao An^{1,2}, Xianying Dai^{1,2}✉, Lansheng Feng³ & Jieming Zheng^{1,2}

We investigated the process parameters of the high temperature MOCVD (HT-MOCVD) numerical model for the AlN growth based on CFD simulation using orthogonal test design. It is believed that high temperature growth condition is favorable for improving efficiency and crystallization quality for AlN film, while the flow field in the HT-MOCVD reactor is closely related to the process parameters, which will affect the uniformity of the film. An independently developed conceptual HT-MOCVD reactor was established for the AlN growth to carry out the CFD simulation. To evaluate the role of the parameters systematically and efficiently on the growth uniformity, the process parameters based on CFD simulation were analyzed using orthogonal test design. The advantages of the range, matrix and variance methods were considered and the results were analyzed comprehensively and the optimal process parameters were obtained as follows, susceptor rotational speed 400 rpm, operating pressure 40 Torr, gas flow rate 50 slm, substrate temperature 1550 K.

Abbreviations

HT-MOCVD	High temperature metal organic chemical vapor deposition
CFD	Computational fluid dynamics
TMAI	Trimethylaluminium

As a wide range of direct bandgap semiconductor material, aluminum nitride (AlN) has been extensively investigated due to its high piezoelectric coefficient and thermal conductivity, and excellent optical and mechanical properties etc^{1–4}, which make it a promising candidate for bulk substrate, blue and ultraviolet photo-detectors and deep ultraviolet LED^{5–9}. Generally, metal organic chemical vapor deposition (MOCVD) is a typical and effective approach to the AlN film growth with TMAI/NH₃ as the gas precursor^{10–15}. At high growth temperature, AlN film can achieved high surface growth rate, and the resultant AlN crystal surface is atomically flat¹⁶. In recent years, some progress of high-quality LED research has been made in experiment, and fluid flow, heat transfer, mass transfer and chemical reactions during the AlN growth have received extensive attention^{17,18}. The effects and mechanisms of varied temperature and pressure on chemical reaction pathways and rate were studied based on Grove theory¹⁹. The effects of flow rate on AlN growth rate was investigated by CFD simulation which found that the film growth rate increased with the increase of hydrogen flow rate²⁰.

Traditional test methods would need a large number of experiments and analyses to obtain effective parametric research. Orthogonal test design is a multi-factor and multi-level multi-factor experimental research method, which is widely used to solve engineering application problems based on mathematical analysis^{21,22}. In this paper, the optimal numerical simulation results can be obtained by the comprehensive optimization design of various parameters of multi-physical fields, a large amount of calculation data will be generated. The test points selected during the orthogonal test design are evenly distributed and uniformly comparable, which have strong representativeness and will meet the demand of comprehensive numerical simulation^{23,24}. This study using an orthogonal test design to find out the best process conditions, the best test results, and gives the scheme of process optimization.

In this paper, the multi-physics fields and process parameters of AlN film growth by HT-MOCVD have been investigated by orthogonal test design. According to the factors and levels, an L₁₆(4⁴) orthogonal array is

¹School of Microelectronics, Xidian University, Xi'an 710071, China. ²State Key Discipline Laboratory of Wide Bandgap Semiconductor Technologies, Xidian University, Xi'an 710071, China. ³School of Mechano-Electronic Engineering, Xi'an 710071, China. ✉email: xydai@xidian.edu.cn

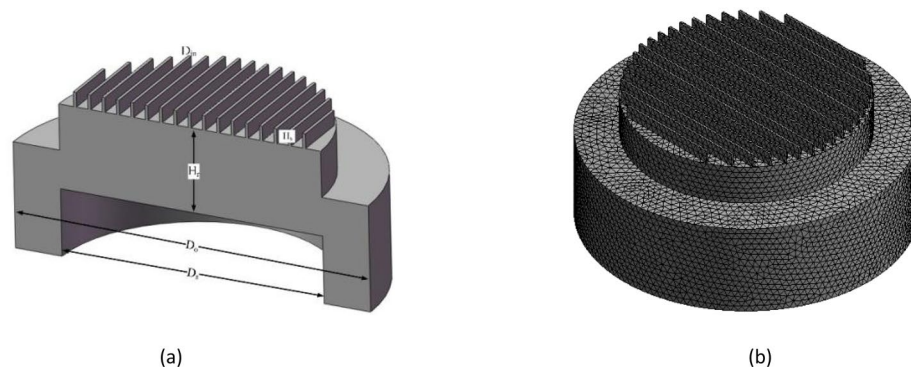


Figure 1. Model and mesh diagram of AlN-HT-MOCVD reactor. (a) Reactor model of the MOCVD reactor; (b) the whole mesh of AlN-MOCVD reactor.

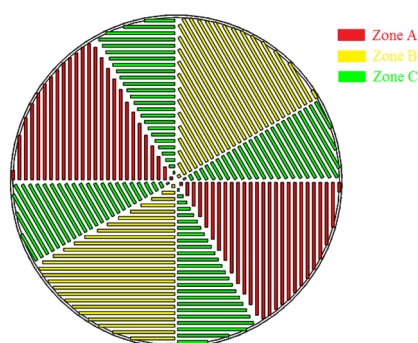


Figure 2. Diagram of isolation device.

employed to quantify the multi-physics fields and process parameters. The influence of process parameters for the optimal film uniformity was analyzed by range, matrix and variance analysis, respectively.

Computation model and methods

Geometry description. Schematic diagram of a specific MOCVD reactor similar to the close-coupled showerhead (CCS) reactor is shown in Fig. 1a. The reactor consisted of the gas inlets, the chamber walls, the susceptor and the gas outlets. The gas inlets are used to transfer the group III metal organic precursors and group V gas hydrides carried by carrier gas (H_2) into the reactor and the precursors gases pass through the chamber to participate in chemical reactions. The whole numerical simulation process is based on a three-dimensional model, which is divided into about one million grids as shown in Fig. 1b. The dimensions of the reactor are described in Fig. 1a which the height (H_r), the width of gas inlet (D_{in}), the susceptor diameter (D_s), the outer wall diameter (D_o) and the reactor height (H_r) are 8 mm, 2 mm, 183 mm, 256 mm and 57.8 mm, respectively. As the reaction chamber is a vertical spray structure. Mixing of gaseous reactants into the reaction chamber may cause the parasitic reactions and produce more complex pre-reactions. Finally, it will affect the uniformity of film deposition. In order to prevent the metallic organic gas source and ammonia from mixing immediately after entering the inlets, we used a zoned isolation device at the inlets. Isolation is done by using carrier gas, which is N_2 and H_2 the inert gas. After the gas source enters the reaction chamber, it will spread in a vertical direction alone under the action of the isolation gas until it is close to the high temperature area of the substrate and then fully mix and react. To a certain extent, the occurrence of parasitic reactions and partial waste of gas sources are avoided. The partition isolation device is shown in Fig. 2, in which area A is TMAI, area B is NH_3 , and area C is N_2 and H_2 .

Orthogonal test design. The orthogonal test design that optimizing the multi-physics fields and process parameters of the AlN growth by HT-MOCVD was divided into several parts: selecting test objectives, evaluating indicators, selecting factors and levels, designing an appropriate orthogonal array, listing test plan and corresponding results, analyzing the test results through range, matrix and variance analysis, and finally finding the optimal combination of factors and levels.

During AlN growth by HT-MOCVD the reactants are TMAI, NH_3 , hydrogen and other gases, and the hydrodynamic behavior and flow field distribution in the reactor will affect the uniformity of the film. The hydrodynamic behavior is closely related to the (A) gas flow rate, (B) operating pressure, (C) substrate temperature, and (D) rotating speed of susceptor. As the test involves 4 degrees of freedom and the complex interaction among

Factors	Level				Unit
	1	2	3	4	
A Total gas flow rate	45	50	55	60	slm
B Operating pressure	40	50	60	70	Torr
C Substrate temperature	1450	1500	1550	1600	K
D Rotating speed	400	600	800	1000	rpm

Table 1. Orthogonal factor and level table.

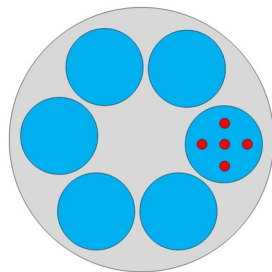


Figure 3. 5-point positions schematic diagram.

them, a large number of experiments are needed to find out the most stable flow field distribution and relatively optimal combination of process parameters.

In the design of orthogonal test, the core issue is to select and identify the factors that may affect the indicators. Therefore, taking no account of the interaction influence among these parameters, the factors can be considered as the variables which correspond to the four free parameters i.e. A, B, C, and D mentioned above. Level, also known as bit-level, corresponding to the factors represented different numerical simulation states. We should consider both the range of parameters and the number of levels to determine the level, so the factors were divided into four continuous levels to represent the variation range. Flow field and heat transfer in the reactor need to be considered and the continuous liquid level should be appropriated. The orthogonal factors and levels are shown in Table 1.

In this study, we have investigated four free parameters and each including four levels. The $L_{16}(4^4)$ orthogonal array was adopted to carry out the optimization combination test. Where L refers to orthogonal array, the 16 represents that the main array has sixteen rows, which indicates 16 cases designed by orthogonal array, the 4 represents that each investigated factors has four levels, and the 5 denotes that the test has five columns, which indicates five factors. As shown in Fig. 3, in order to analyze the influence of the four factors on the three indicators, 5 points on the substrate were selected according to the 5 point principle of wafer uniformity. The variance of the simulation results is calculated as

$$S^2 = \frac{\sum_{i=1}^n (x_i - m)^2}{(n - 1)} \quad (1)$$

where x_i is the data of one point, m is the average value of x_i , and n is the number of data.

As shown in Table 2, the first column lists the numbers from 1 to 16, representing the 16 simulation cases. Columns 2 to 5 represent levels of different factors, i.e. A, B, C and D. Considering that the numerical simulation in this study involves four changing factors, the last column in the table is error evaluation, namely error term. In Table 1, each row in the table corresponds to a growth condition, where the numbers “1, 2, 3, 4” represent the different levels of each factor. For example, the 5th case corresponds to a combination of 2nd level of A, the 1st level of B, the 2ed level of C and the 3rd level of D. The right columns on the right side of the table list the indicators, namely the density variance, pressure variance, and temperature variance for each case. During this study the sixteen simulation cases were investigated using CFD numerical method and the results of the 14th case are shown in Figs. 4 and 5.

According to the design above, for any column, all four levels were participated and occur with the same frequency. Two columns contain any possible combination of levels and the occurrences are equal. Each layer of a factor is equal to the combination of factors of the other layers, indicating that the horizontal configuration between any two columns is consistent.

Results and discussion

Range analysis. Judging the order and optimal level of each factor by the average value of each factor based on the orthogonal test design. The judgment methods are as follows: (1) K_1, K_2, K_3, K_4 represent the average value of each factor at each level. By comparing the mean of the levels to determine the factors of the optimal level, the smaller the \bar{K}_i , the smaller the variance of the experimental results, the better the uniformity caused by the

Case	A	B	C	D	Error term	Density variance	Pressure variance	Temperature variance
1	1	1	1	1	1	4.4211×10^{-11}	6.0372×10^{-8}	1.3966×10
2	1	2	2	2	2	1.3856×10^{-10}	3.3669×10^{-7}	1.1943×10
3	1	3	3	3	3	3.9001×10^{-10}	9.0930×10^{-7}	1.0605×10
4	1	4	4	4	4	4.2459×10^{-10}	1.6954×10^{-6}	1.5956×10
5	2	1	2	3	4	8.0444×10^{-11}	6.4854×10^{-7}	1.1331×10
6	2	2	1	4	3	2.6294×10^{-10}	1.4698×10^{-6}	0.9650×10
7	2	3	4	1	2	1.1161×10^{-10}	8.7931×10^{-8}	1.6038×10
8	2	4	3	2	1	2.0482×10^{-10}	1.0645×10^{-7}	1.3949×10
9	3	1	3	4	2	9.3821×10^{-11}	1.2373×10^{-6}	1.1044×10
10	3	2	1	3	1	1.9523×10^{-10}	7.2691×10^{-7}	0.9417×10
11	3	3	4	2	4	2.1107×10^{-10}	3.2333×10^{-7}	1.3227×10
12	3	4	2	1	3	2.0932×10^{-10}	1.0082×10^{-7}	1.2661×10
13	4	1	4	2	3	5.0425×10^{-11}	2.0195×10^{-7}	1.5945×10
14	4	2	3	13	4	6.7071×10^{-11}	5.8788×10^{-8}	1.5671×10
15	4	3	2	4	1	4.5579×10^{-10}	1.3709×10^{-6}	1.2380×10
16	4	4	1	3	2	4.8599×10^{-10}	6.8550×10^{-7}	1.1808×10

Table 2. $L_{16}(4^4)$ orthogonal designed scheme and results.

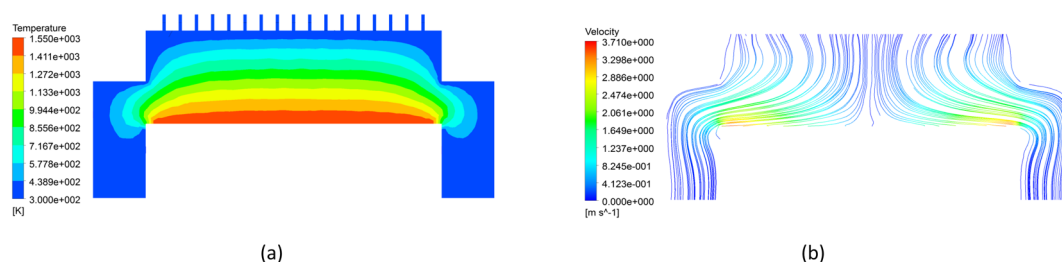


Figure 4. Distributions of fields (a) temperature and (b) velocity magnitude in the reactor.

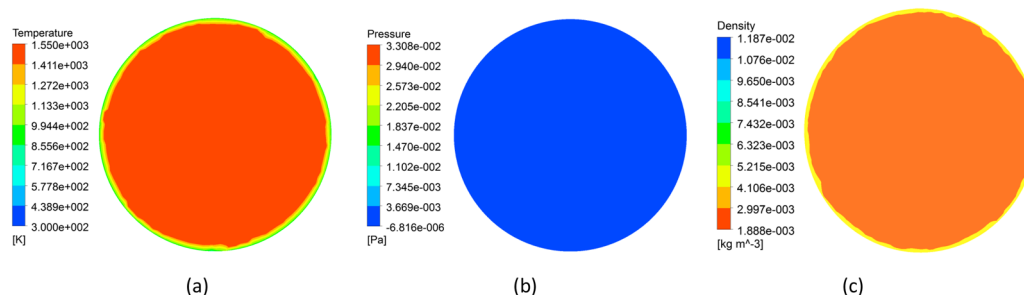


Figure 5. Distributions of fields on the substrate. (a) temperature (b) pressure (c) density.

case. (2) Range $R = \max \{K_1, K_2, K_3, K_4\} - \min \{K_1, K_2, K_3, K_4\}$ indicates the influence of various factors. The large range indicates that the horizontal variation of this factor has a great influence on the experimental result which is the main factor. The range of error term indicates the error caused by the random. If the range of error term is large, an interaction between various factors exists. Through the simulation of 16 orthogonal test cases, the order of each factor and the optimal level of density distribution, pressure distribution and temperature distribution were obtained. As the Table 3 shows, the range of error term in the three indicators is smaller than that of other factors, indicating that the interaction among factors is weak. Therefore, the orthogonal test design is reasonable and there is no need for interactive design.

As the range of B (2.6395×10^{-10}) > the range of D (2.0123×10^{-10}) > the range of C (1.1939×10^{-10}) > the range of A (9.9865×10^{-11}), which affects the density distribution is B, D, C, A. Therefore, the optimal level combination of density distribution is $B_1-D_1-C_3-A_2$. Similarly, the optimal level combination of pressure distribution and temperature distribution is $D_1-A_2-C_4-B_1$ and $C_1-D_3-A_3-B_2$.

Index	Indicator	Factor				
		A	B	C	D	Error term
Density distribution	\bar{K}_1	2.4934×10^{-10}	6.7225×10^{-11}	2.4709×10^{-10}	1.0805×10^{-10}	2.2501×10^{-10}
	\bar{K}_2	1.6495×10^{-10}	1.6595×10^{-10}	2.2103×10^{-10}	1.5122×10^{-10}	1.9994×10^{-10}
	\bar{K}_3	1.7736×10^{-10}	2.9212×10^{-10}	1.8893×10^{-10}	2.8792×10^{-10}	2.2817×10^{-10}
	\bar{K}_4	2.6482×10^{-10}	3.3118×10^{-10}	3.0832×10^{-10}	3.0928×10^{-10}	1.9579×10^{-10}
	R	9.9865×10^{-11}	2.6395×10^{-10}	1.1939×10^{-10}	2.0123×10^{-10}	3.2380×10^{-11}
	Order	B ₁ -D ₁ -C ₃ -A ₂				
Pressure distribution	\bar{K}_1	7.5043×10^{-7}	5.3705×10^{-7}	7.3565×10^{-7}	7.6979×10^{-8}	5.6615×10^{-7}
	\bar{K}_2	5.7819×10^{-7}	6.4805×10^{-7}	6.1423×10^{-7}	2.4210×10^{-7}	5.8686×10^{-7}
	\bar{K}_3	5.9710×10^{-7}	6.7286×10^{-7}	5.7797×10^{-7}	7.4256×10^{-7}	6.7048×10^{-7}
	\bar{K}_4	5.7927×10^{-7}	6.4703×10^{-7}	5.7714×10^{-7}	1.4433×10^{-6}	6.8150×10^{-7}
	R	1.7224×10^{-7}	1.3581×10^{-7}	1.5851×10^{-7}	1.3664×10^{-6}	1.1535×10^{-7}
	Order	D ₁ -A ₂ -C ₄ -B ₁				
Temperature distribution	\bar{K}_1	13.1174	13.0717	11.2102	14.5840	12.4282
	\bar{K}_2	12.7422	11.6702	12.0788	13.7660	12.7081
	\bar{K}_3	11.5874	13.0626	12.8173	10.7903	12.2153
	\bar{K}_4	13.9510	13.5935	15.2916	12.2576	14.0463
	R	2.3637	1.9232	4.0814	3.7937	1.8310
	Order	C ₁ -D ₃ -A ₃ -B ₂				

Table 3. Optimal combination of process parameters with single index.

Matrix analysis. The order of the factors and the optimal level were judged by the range analysis, while the weight of each factor and level should be analyzed to determine the optimal combination using the matrix analysis. As the index layer, factor layer and level layer are the three-layer structural models of the orthogonal test, we defined 1, index layer matrix: including m factors, each factor is divided into n levels, and the average index of the j level of factor A_i is K_{ij}. The surface of the film is expected to be uniform, and the matrix was

$$M = \begin{pmatrix} K_{11} & 0 & \dots & 0 \\ K_{12} & 0 & \dots & 0 \\ \vdots & \vdots & \ddots & \vdots \\ 0 & 0 & 0 & K_{mn} \end{pmatrix}. \tag{2}$$

Definition 2, factor layer matrix, $T_i = 1 / \sum_{j=1}^n K_{ij}$, matrix T was established as

$$T = \begin{pmatrix} T_1 & 0 & \dots & 0 \\ 0 & T_2 & \dots & 0 \\ \vdots & \vdots & \ddots & \vdots \\ 0 & 0 & 0 & T_m \end{pmatrix}. \tag{3}$$

Definition 3, level layer matrix, the range of A_i is s_i, $S_i = s_i / \sum_{i=1}^m s_i$, matrix S was established as

$$S^T = (S_1 \ S_2 \ \dots \ S_m) \tag{4}$$

The range analysis method of multi-index orthogonal experiment is summarized.

Step 1 Find the K matrix, T matrix and S matrix of each factor, and then calculate the weight matrix k_i (i = 1, ..., m).

Step 2: Take the mean matrix of the m matrices $\sum_{i=1}^m k_i / m$ as follows

$$k^T = (A_{11} \ \dots \ A_{1n} \ \dots \ A_{m1} \ \dots \ A_{mn}) \tag{5}$$

where A_{ij} (i = 1 ... M, j = 1 ... N) indicator values corresponding to the jth level of the first factor.

Step 3 According to the requirements of the test for each index, find out the level j corresponding to the maximum or minimum value of each A_i in the K matrix, regard it as the optimal level of the corresponding factors, and then find out the optimal level combination of all factors.

According to the above calculation steps, the weight matrix of the temperature distribution is calculated as follows

$$T_3 = \begin{pmatrix} 0.313 & 0 & 0 & 0 \\ 0 & 0.312 & 0 & 0 \\ 0 & 0 & 0.315 & 0 \\ 0 & 0 & 0 & 0.315 \end{pmatrix} \tag{6}$$

$$S_3 = \begin{pmatrix} 0.194 \\ 0.158 \\ 0.336 \\ 0.312 \end{pmatrix} \tag{7}$$

$$M_3 = \begin{pmatrix} 0.076 & 0 & 0 & 0 \\ 0.078 & 0 & 0 & 0 \\ 0.086 & 0 & 0 & 0 \\ 0.072 & 0 & 0 & 0 \\ 0 & 0.077 & 0 & 0 \\ 0 & 0.086 & 0 & 0 \\ 0 & 0.077 & 0 & 0 \\ 0 & 0.074 & 0 & 0 \\ 0 & 0 & 0.089 & 0 \\ 0 & 0 & 0.083 & 0 \\ 0 & 0 & 0.078 & 0 \\ 0 & 0 & 0.065 & 0 \\ 0 & 0 & 0 & 0.069 \\ 0 & 0 & 0 & 0.073 \\ 0 & 0 & 0 & 0.093 \\ 0 & 0 & 0 & 0.082 \end{pmatrix} \tag{8}$$

$$k_3 = M_3 T_3 S_3 = \begin{pmatrix} 0.0046 \\ 0.0048 \\ 0.0052 \\ 0.0044 \\ 0.0038 \\ 0.0042 \\ 0.0038 \\ 0.0036 \\ 0.0094 \\ 0.0088 \\ 0.0083 \\ 0.0069 \\ 0.0067 \\ 0.0071 \\ 0.0091 \\ 0.0080 \end{pmatrix} \tag{9}$$

$$k_1 = \begin{pmatrix} 0.1141 \\ 0.1723 \\ 0.1604 \\ 0.1074 \\ 1.5688 \\ 0.6356 \\ 0.3610 \\ 0.3185 \\ 0.1207 \\ 0.1350 \\ 0.1580 \\ 0.0968 \\ 0.6142 \\ 0.4390 \\ 0.2305 \\ 0.2146 \end{pmatrix} \tag{10}$$

Similarly, the weight matrix K_2 of the density distribution and the weight matrix K_3 of the pressure distribution are calculated. Finally, the weight matrix which affects the index is obtained

Index	Factor	S	f	V	F_a	F_θ	Significance level
Density distribution	A	1.8949×10^{-21}	3	6.3165×10^{-22}	9.04	$F_{0.10}(3,3) = 5.39$	Significant
	B	1.0921×10^{-20}	3	3.6405×10^{-21}	52.09	$F_{0.05}(3,3) = 9.28$	Significant
	C	1.9196×10^{-21}	3	6.3986×10^{-22}	9.16	$F_{0.025}(3,3) = 15.4$	Insignificant
	D	7.4274×10^{-21}	3	2.4758×10^{-21}	35.43	$F_{0.005}(3,3) = 47.5$	Insignificant
	e	2.0966×10^{-22}	3	6.9886×10^{-23}			
Pressure distribution	A	5.1967×10^{-15}	3	1.7322×10^{-15}	2.04	$F_{0.10}(3,3) = 5.39$	Insignificant
	B	2.7591×10^{-15}	3	9.1969×10^{-16}	1.09	$F_{0.05}(3,3) = 9.28$	Insignificant
	C	4.2141×10^{-15}	3	1.4047×10^{-15}	1.66	$F_{0.025}(3,3) = 15.4$	Insignificant
	D	2.8261×10^{-13}	3	9.4203×10^{-14}	111.1	$F_{0.005}(3,3) = 47.5$	Significant
	e	2.5430×10^{-15}	3	8.4768×10^{-16}			
Temperature distribution	A	0.7224	3	2.4080×10^{-1}	1.42	$F_{0.10}(3,3) = 5.39$	Insignificant
	B	0.5097	3	1.6991×10^{-1}	1.00	$F_{0.05}(3,3) = 9.28$	Insignificant
	C	2.3116	3	7.7052×10^{-1}	4.55	$F_{0.025}(3,3) = 15.4$	Insignificant
	D	2.1098	3	7.0325×10^{-1}	4.15	$F_{0.005}(3,3) = 47.5$	Insignificant
	e	0.5080	3	1.6934×10^{-1}			

Table 4. Analysis of variance of orthogonal experiment.

$$k_2 = \begin{pmatrix} 0.0081 \\ 0.0105 \\ 0.0102 \\ 0.0105 \\ 0.0089 \\ 0.0074 \\ 0.0071 \\ 0.0074 \\ 0.0076 \\ 0.0091 \\ 0.0097 \\ 0.0097 \\ 1.8555 \\ 0.5900 \\ 0.1923 \\ 0.0990 \end{pmatrix} \quad (11)$$

$$k = \frac{k_1 + k_2 + k_3}{3} = \begin{pmatrix} 0.0422 \\ 0.0624 \\ 0.0585 \\ 0.0406 \\ 0.5272 \\ 0.2159 \\ 0.1240 \\ 0.1100 \\ 0.0460 \\ 0.0510 \\ 0.0587 \\ 0.0379 \\ 0.8254 \\ 0.3454 \\ 0.1441 \\ 0.1073 \end{pmatrix} \quad (12)$$

Based on the above calculation and analysis, the optimum combination is $D_1-B_1-A_2-C_3$. The optimum process parameters for the AlN growth by HT-MOCVD are as follows, the susceptor rotational speed 400 rpm, the operating pressure 40 Torr, the gas flow rate 50 slm, the substrate temperature 1550 K.

Variance analysis

The matrix analysis method can obtain the optimum process parameters, while the cause of the difference of experiment results at different levels of factors is not clear. The analysis of variance can not only give an accurate estimate of the impact of each factor on the test results, but also provide a criterion to judge whether the effect of the factors examined is significant. We performed variance analysis and the results are shown in Table 4.

In the variance analysis of orthogonal test, the variance of error term is used as the estimation of test error. The formulas used in variance analysis are as follows

$$S = \sum_{i=1}^K \frac{T_i^2}{K} - \frac{T^2}{n} \quad (13)$$

$$f = K - 1 \quad (14)$$

$$V = \frac{S}{f} \quad (15)$$

$$F_\theta = \frac{V_f}{V_\theta} \quad (16)$$

where S is the sum of deviation squares, K is the total number of factors, n is the total number of experiments, T_i is the sum of the data corresponding to level i , T is the sum of all experimental data, f is the degree of freedom of factors, V is the mean square, F_θ is the ratio of F , V_f is the mean square of factors, and V_θ is the mean square of errors.

According to the theory of mathematical statistics, if F_a is greater than F_θ , it is considered that this factor has a significant effect on the results; if F_a is less than F_θ , it is considered that this factor has no significant effect on the results. As shown in Table 4, for density distribution, according to F_θ , the order of factors can be determined as $B \rightarrow D \rightarrow C \rightarrow A$, in which the F_θ of pressure is much larger than $F_{0.05}(3,3)$, and the pressure factor is very significant; The pressure distribution is determined by F_θ to determine the order of factors as $D \rightarrow A \rightarrow C \rightarrow B$. The temperature distribution is determined by F_θ to determine the order of factors as $C \rightarrow D \rightarrow A \rightarrow B$. Through the evaluation of variance method, the optimal parameters obtained were verified, and the criterion to judge whether the effect of the factors examined is significant can provide theoretical guidance for optimization of process parameters during HT-MOCVD growth.

Conclusion

In this paper, an optimized multi-physical field numerical model was established for the AlN growth by high temperature MOCVD (HT-MOCVD) based on CFD simulation and the influences of the process parameters on the AlN growth uniformity were investigated carefully based on the orthogonal test design. Firstly, the orthogonal test design takes the susceptor rotational speed, operating pressure, gas flow rate, substrate temperature as factors, and the density field distribution, pressure field distribution, temperature field distribution as indicators. Then, the data of 5 points on the surface were extracted to quantify the film uniformity. Finally, the results were analyzed by range, matrix and variance methods considering the influence of process parameters on film uniformity. The optimum process parameters of this three-dimensional reactor for the AlN growth by HT-MOCVD were obtained as follows: the susceptor rotational speed 400 rpm, operating pressure 40 Torr, gas flow rate 50 slm, substrate temperature 1550 K.

Data availability

The datasets used and/or analysed during the current study are available from the corresponding author on reasonable request.

Received: 18 January 2021; Accepted: 30 March 2021

Published online: 23 April 2021

References

- Kinoshita, T. *et al.* *Appl. Phys. Express* **8**, 061003 (2015).
- Inoue, S., Naoki, T., Kinoshita, T., Obata, T. & Yanagi, H. Light extraction enhancement of 265 nm deep-ultraviolet light-emitting diodes with over 90 mW output power via an AlN hybrid nanostructure. *Appl. Phys. Lett.* **106**, 131104 (2015).
- Faria, F. A. *et al.* Low temperature AlN growth by MBE and its application in HEMTs. *J. Cryst. Growth* **425**, 133–137 (2015).
- Taniyasu, Y., Kasu, M. & Makimoto, T. An aluminum nitride light-emitting diode with a wavelength of 210 nanometres. *Nature* **441**, 325–328 (2006).
- Lin, W. T., Meng, L., Chen, G. & Liu, H. Epitaxial growth of cubic AlN films on (100) and (111) silicon by pulsed laser ablation. *Appl. Phys. Lett.* **66**, 2066 (1995).
- Cheng, H. *et al.* AlN films deposited under various nitrogen concentrations by RF reactive sputtering. *J. Cryst. Growth* **254**, 46 (2003).
- Ristoscu, C., Ducu, C., Socol, G., Craciunoiu, F. & Mihailescu, I. N. Structural and optical characterization of AlN films growth by pulsed laser deposition. *Appl. Surf. Sci.* **248**, 411 (2005).
- Schowalter, L. J. *et al.* Epitaxial growth of AlN and $Al_{0.5}Ga_{0.5}N$ layers on aluminum nitride substrates. *J. Cryst. Growth* **211**, 78–81 (2000).
- Ikenaga, M. *et al.* Quantum chemical study of gas-phase reactions of trimethylaluminum and triethylaluminum with ammonia in III–V nitride semiconductor crystal growth. *J. Cryst. Growth* **237**(1), 936–941 (2002).
- Mihopoulos, T. G., Gupta, V. & Jensen, K. F. A reaction-transport model for AlGaIn MOVPE growth. *J. Cryst. Growth* **195**(1–4), 733–739 (1998).
- Ohba, Y., Yoshida, H. & Sato, R. Growth of high-quality AlN, GaN and AlGaIn with atomically smooth surfaces on sapphire substrates. *Jpn. J. Appl. Phys.* **36**, L1565 (1997).
- Nakamura, K. *et al.* Quantum chemical study of parasitic reaction in III–V nitride semiconductor crystal growth. *J. Organomet. Chem.* **611**(1), 514–524 (2000).
- Creighton, J. R., Wang, G. T. & Coltrin, M. E. Fundamental chemistry and modeling of group-III nitride MOVPE. *J. Cryst. Growth* **298**, 2–7 (2007).

14. Nakamura, K., Hirako, A. & Ohkawa, K. Analysis of pulsed injection of precursors in AlN-MOVPE growth by computational fluid simulation. *Phys. Status Solidi C* **7**, 2268–2271 (2010).
15. Uchida, T., Kusakabe, K. & Ohkawa, K. Influence of polymer formation on metalorganic vapor-phase epitaxial growth of AlN. *J. Cryst. Growth* **304**, 133–140 (2007).
16. Tsai, C. L., Liu, H. H., Chen, J. W. *et al.* Improving the light output power of DUV-LED by introducing the intrinsic last quantum barrier interlayer on the high-quality AlN template, in *International Symposium on Next-generation Electronics* (IEEE, 2016).
17. Enslin, J. *et al.* Metamorphic Al_{0.5}Ga_{0.5}N: Si on AlN/sapphire for the growth of UVB LEDs. *J. Cryst. Growth* **464**, 185–189 (2017).
18. Lee, B. R. *et al.* ITO/Ag/AlN/Al₂O₃ multilayer electrodes with conductive channels: application in ultraviolet light-emitting diodes. *J. Alloy. Compd.* **741**, 21–27 (2018).
19. Pu, K. *et al.* A kinetics model for MOCVD deposition of AlN film based on Grove theory. *J. Cryst. Growth* **478**, S0022024817304967 (2017).
20. Bao, Q. *et al.* Effect of hydrogen carrier gas on AlN and AlGaIn growth in AMEC Prismo D-Blue MOCVD platform. *J. Cryst. Growth* **419**, 52–56 (2015).
21. Zhang, Z. *et al.* Influencing factors of GaN growth uniformity through orthogonal test analysis. *Appl. Therm. Eng.* **91**, 53–61 (2015).
22. Xiang, P. *et al.* Orthogonal design for fabrication of ZnO thin films by MOCVD. *Semicond. Optoelectron.* **17**(7), 23–25 (2008).
23. Liu, Y. W. *et al.* Parameter study of the injection configuration in a zero boil-off hydrogen storage tank using orthogonal test design. *Appl. Therm. Eng.* **109**, 283–294 (2016).
24. Cui, W. *et al.* Investigation on process parameters of electrospinning system through orthogonal experimental design. *J. Appl. Polym. Sci.* **103**(5), 3105–3112 (2007).

Author contributions

X.D. designed this project. J.A. performed the calculations, analyzed the calculated results and wrote the original manuscript. J.Z. checked the calculation results and modified the manuscript. L.F. modified the manuscript. All authors discussed the results and worked on the final manuscript.

Funding

The National Key R&D Program of China (Grant No. 2017YFB0404202), and the 111 Project (No. B12026).

Competing interests

The authors declare no competing interests.

Additional information

Correspondence and requests for materials should be addressed to X.D.

Reprints and permissions information is available at www.nature.com/reprints.

Publisher's note Springer Nature remains neutral with regard to jurisdictional claims in published maps and institutional affiliations.



Open Access This article is licensed under a Creative Commons Attribution 4.0 International License, which permits use, sharing, adaptation, distribution and reproduction in any medium or format, as long as you give appropriate credit to the original author(s) and the source, provide a link to the Creative Commons licence, and indicate if changes were made. The images or other third party material in this article are included in the article's Creative Commons licence, unless indicated otherwise in a credit line to the material. If material is not included in the article's Creative Commons licence and your intended use is not permitted by statutory regulation or exceeds the permitted use, you will need to obtain permission directly from the copyright holder. To view a copy of this licence, visit <http://creativecommons.org/licenses/by/4.0/>.

© The Author(s) 2021